Università degli Studi di Padova

Axion Helioscopes as Solar Thermometers

Sebastian Hoof

Based on [2306.00077] with J. Jaeckel & L. J. Thormaehlen

Axions++, LAPTh Annecy

27 September 2023

Funded by
the European Union

msca_axitools

Recap: axion helioscopes

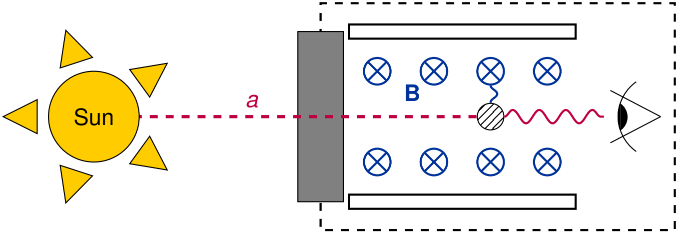

- Axions produced in the Sun travel to Earth, convert into photons in a B-field inside an opaque tube [Talk by J. Vogel (Tue)]

➽ Track the Sun with X-ray detectors [Talks by L. Gastaldo, J. von Oy (Tue)]

- Signal prediction: need solar model, axion production rates

Recap: interesting points about IAXO

IAXO can…

- … probe more realistic QCD axion models than CAST!
- … determine mass & couplings[1811.09278, 1811.09290], simultaneously distinguish QCD axion and solar models[2101.08789]
- … measure solar metallicities[1908.10878, 2101.08789]
- … solar B-field (profiles),[2005.00078, 2006.12431, 2010.06601]
- … measure the solar temperature profile [2306.00077]

Recap: interesting points about IAXO

IAXO can…

… probe more realistic QCD axion models than CAST!

… determine mass & couplings[1811.09278, 1811.09290], simultaneously distinguish QCD axion and solar models[2101.08789]

… measure solar metallicities[1908.10878, 2101.08789]

… solar *B*-field (profiles),[2005.00078, 2006.12431, 2010.06601]

… *measure the solar temperature profile*[2306.00077]

➽ ***Post-discovery multi-messenger physics with IAXO***

Axion interactions inside the Sun

$$\mathcal{L}_{\rm ALP} = \frac{(\partial_\mu a)^2}{2} - \underbrace{\frac{m_a^2 a^2}{2}}_{m_a \ll T_\odot} - \frac{g_{a\gamma}}{4}\, a F\widetilde{F} + \frac{g_{ae}}{2m_e}(\partial_\mu a)\,\bar{e}\gamma^\mu\gamma^5 e \underbrace{+ \mathcal{L}_{\rm nucl} +}_{[2111.06407]} \mathcal{L}_{\cancel{CP}}$$

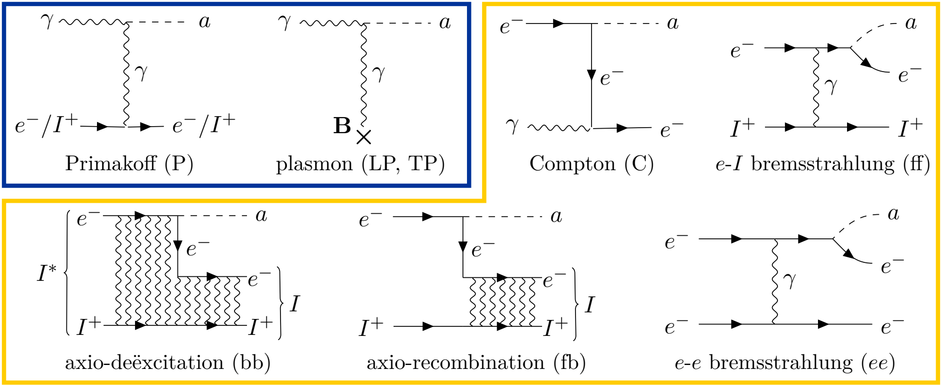

Works by Raffelt+, Redondo, . . . ; see [2101.08789] for refs

Solar axion flux uncertainties

10,000 Monte Carlo sims of low-Z (AGSS09) & high-Z (GS98) solar models[astro-ph/0511337 + A. Serenelli update] to estimate uncertainties[2101.08789]

Primakoff fluxes

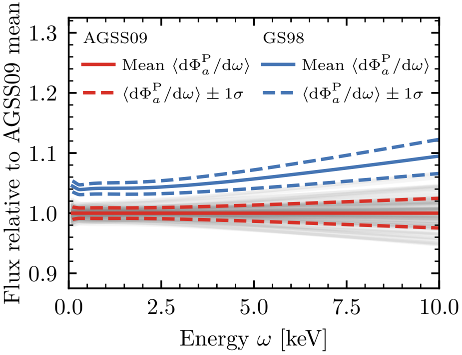

ABC fluxes

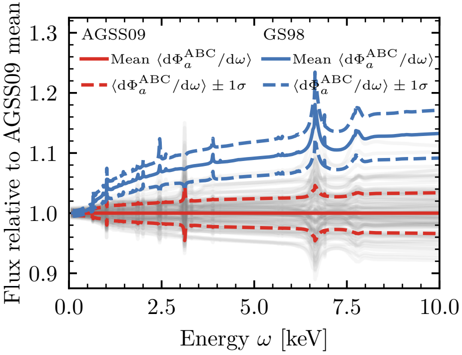

Solar axion flux uncertainties

10,000 Monte Carlo sims of low-Z (AGSS09) & high-Z (GS98) solar models[astro-ph/0511337 + A. Serenelli update] to estimate uncertainties[2101.08789]

Primakoff fluxes

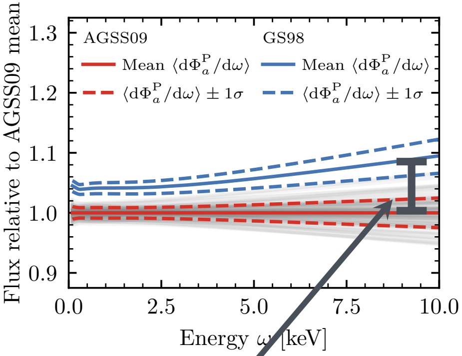

ABC fluxes

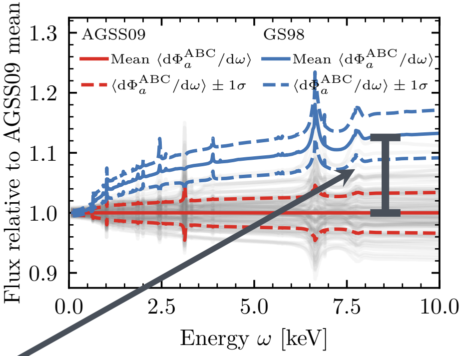

Systematic shift between low-Z and high-Z models (metallicity problem)

Solar axion flux uncertainties

10,000 Monte Carlo sims of low-Z (AGSS09) & high-Z (GS98) solar models[astro-ph/0511337 + A. Serenelli update] to estimate uncertainties[2101.08789]

Primakoff fluxes

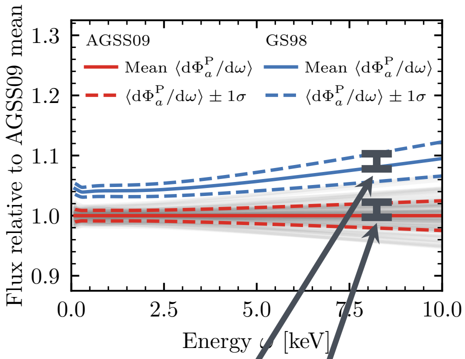

ABC fluxes

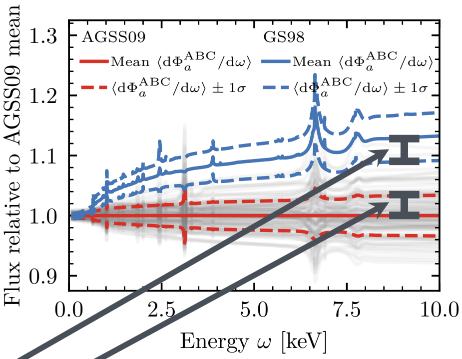

Statistical fluctuations; similar for low-Z and high-Z models, smaller than systematics

Solar metallicity problem solved?

A&A 661, A140 (2022)
https://doi.org/10.1051/0004-6361/202142971

Astronomy & Astrophysics

Observational constraints on the origin of the elements

IV. Standard composition of the Sun

Ekaterina Magg[1], Maria Bergemann[1,5], Aldo Serenelli[2,3,1], Manuel Bautista[4], Bertrand Plez[7], Ulrike Heiter[6], Jeffrey M. Gerber[1], Hans-Günter Ludwig[8], Sarbani Basu[9], Jason W. Ferguson[10], Helena Carvajal Gallego[11], Sébastien Gamrath[11], Patrick Palmeri[11], and Pascal Quinet[11,12]

- New composition: MB22[2203.02255]
- First to reproduce sound velocity profile $c(r)$ with both photospheric and meteoritic abundances? (However: potential issues?[2308.13368])

Solar metallicity problem solved?

A&A 661, A140 (2022)
https://doi.org/10.1051/0004-6361/202142971

Astronomy & Astrophysics

Observational constraints on the origin of the elements

IV. Standard composition of the Sun

Ekaterina Magg[1], Maria Bergemann[1,5], Aldo Serenelli[2,3,1], Manuel Bautista[4], Bertrand Plez[7], Ulrike Heiter[6], Jeffrey M. Gerber[1], Hans-Günter Ludwig[8], Sarbani Basu[9], Jason W. Ferguson[10], Helena Carvajal Gallego[11], Sébastien Gamrath[11], Patrick Palmeri[11], and Pascal Quinet[11,12]

- New composition: MB22[2203.02255]
- First to reproduce sound velocity profile $c(r)$ with both photospheric and meteoritic abundances? (However: potential issues?[2308.13368])

➽ Benefits of our open-source code: re-compute all fluxes for models based on new compositions once available

Primakoff flux on the solar disc

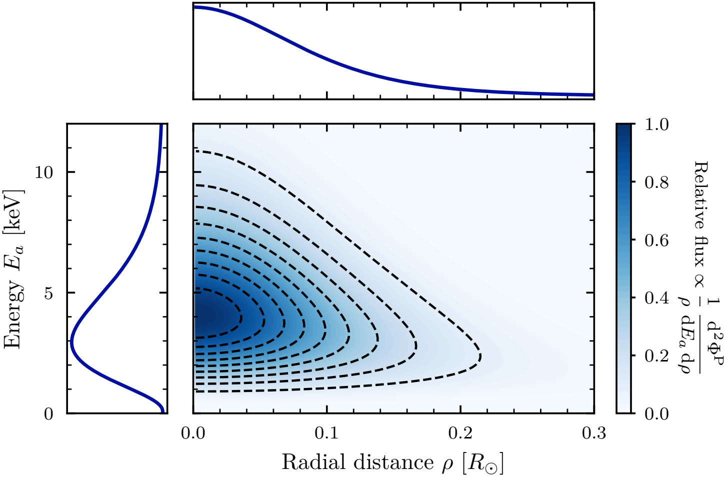

Primakoff flux: dominant for KSVZ, 50% (99%) of the flux is contained within about $0.15\,\mathrm{R}_\odot$ ($0.5\,\mathrm{R}_\odot$).

The solar axion image

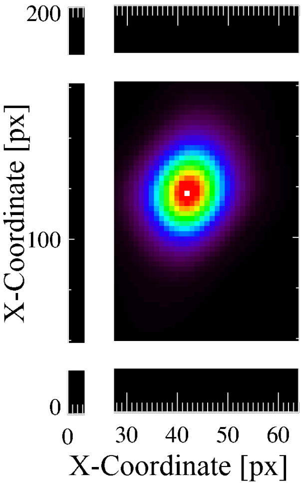

- *Left:* simulated axion image in CAST helioscope[hep-ex/0702006]

The solar axion image

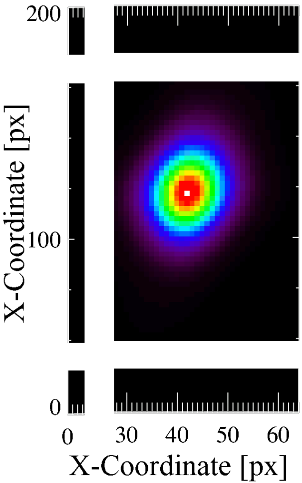

- *Left:* simulated axion image in CAST helioscope[hep-ex/0702006]
- ≈ spherically symmetric thanks to great X-ray optics
- Also: photon counting detectors with high number of pixels

The solar axion image

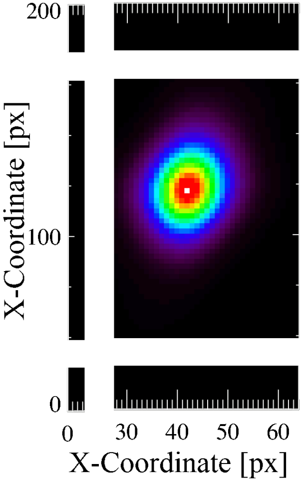

- *Left:* simulated axion image in CAST helioscope[hep-ex/0702006]
- $\approx$ spherically symmetric thanks to great X-ray optics
- Also: photon counting detectors with high number of pixels

➽ Estimate photon counts in rings about the centre of the signal region to obtain radial information

The solar axion image

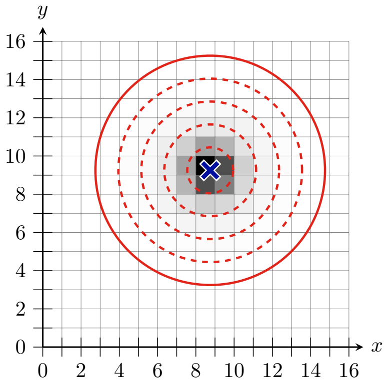

- *Left:* expected signal in IAXO. We use 128 $\times$ 128 pixels, 20 radial and 4 spectral bins

The solar axion image

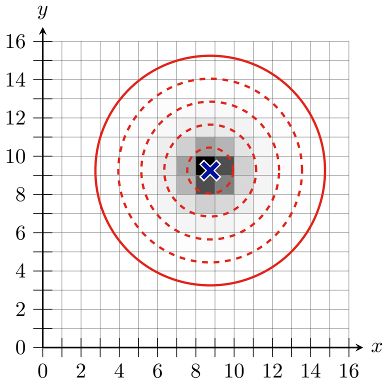

- *Left:* expected signal in IAXO. We use 128 $\times$ 128 pixels, 20 radial and 4 spectral bins
- Many pixels: photon counts/pixel $\approx$ equally distributed, integrate flux over radial bins

➽ Generate 1000 pseudodata sets for IAXO, “invert” solar axion image, fit axion and solar model parameters

The (simplified) Primakoff production rate

$$\Gamma^{\mathsf{P}}(E_a) = \frac{g_{a\gamma}^2\,\kappa_{\mathsf{s}}^2\,T}{32\pi}\left[\left(1+\frac{\kappa_{\mathsf{s}}^2}{4E_a^2}\right)\log\left(1+\frac{4E_a^2}{\kappa_{\mathsf{s}}^2}\right)-1\right]\frac{2}{\mathrm{e}^{E_a/T}-1}$$

The (simplified) Primakoff production rate

$$\Gamma^{\mathrm{P}}(E_a) = \frac{g_{a\gamma}^2\,\kappa_{\mathrm{s}}^2\,T}{32\pi}\left[\left(1+\frac{\kappa_{\mathrm{s}}^2}{4E_a^2}\right)\log\left(1+\frac{4E_a^2}{\kappa_{\mathrm{s}}^2}\right)-1\right]\frac{2}{\mathrm{e}^{E_a/T}-1}$$

- Only depends on $T(r)$, $\kappa_{\mathrm{s}}(r)$ (local) and $g_{a\gamma}$ (global quantity)
- Ignores e^- degeneracy and other corrections (few %)

The (simplified) Primakoff production rate

$$\Gamma^{\mathsf{P}}(E_a) = \frac{g_{a\gamma}^2\,\kappa_{\mathsf{s}}^2\,T}{32\pi}\left[\left(1+\frac{\kappa_{\mathsf{s}}^2}{4E_a^2}\right)\log\left(1+\frac{4E_a^2}{\kappa_{\mathsf{s}}^2}\right)-1\right]\frac{2}{\mathrm{e}^{E_a/T}-1}$$

- Only depends on $T(r)$, $\kappa_{\mathsf{s}}(r)$ (local) and $g_{a\gamma}$ (global quantity)
- Ignores e^- degeneracy and other corrections (few %)
- ➽ Can break parameter degeneracies with spectral information!

$$\bar{n}_{i,j} \propto \int_{\rho_i}^{\rho_{i+1}} \mathrm{d}\rho \int_{\rho}^{1} \mathrm{d}r\, \frac{r\,\rho}{\sqrt{r^2-\rho^2}} \underbrace{\left(\int_{\omega_j}^{\omega_{j+1}} \mathrm{d}\omega\, \frac{\omega^2}{2\pi^2}\,\Gamma^{\mathsf{P}}(r,\,\omega)\right)}_{\equiv \bar{\Gamma}_j^{\mathsf{P}}(r)}$$

A simple reconstruction example

Piecewise-constant interpolation for $\bar{\Gamma}^{\mathsf{P}}_j$

$$\bar{\Gamma}^{\mathsf{P}}_j(r) = \sum_i \underbrace{\left(\int_{\omega_j}^{\omega_{j+1}} \mathrm{d}\omega \, \frac{\omega^2}{2\pi^2} \, \Gamma^{\mathsf{P}}(r_i, \, \omega) \right)}_{\gamma_{i,j}} \, \Theta(r - r_i) \, \Theta(r_{i+1} - r)$$

A simple reconstruction example

Piecewise-constant interpolation for $\bar{\Gamma}^{\mathrm{P}}_j$ + compute the $\bar{n}_{i,j}$ integral

$$\bar{\Gamma}^{\mathrm{P}}_j(r) = \sum_i \underbrace{\left(\int_{\omega_j}^{\omega_{j+1}} \mathrm{d}\omega \, \frac{\omega^2}{2\pi^2} \, \Gamma^{\mathrm{P}}(r_i, \, \omega) \right)}_{\gamma_{i,j}} \Theta(r - r_i) \, \Theta(r_{i+1} - r)$$

$$\begin{aligned} \bar{n}_{i,j} &\propto \int_{r_i}^{r_{i+1}} \mathrm{d}\rho \, \rho \sum_{k=1}^{n_\rho} \int_\rho^1 \mathrm{d}r \, \frac{r}{\sqrt{r^2 - \rho^2}} \, \gamma_{k,j} \, \Theta(r - r_k) \, \Theta(r_{k+1} - r) \\ &= \frac{1}{3} \left[\gamma_{i,j} \, \Delta^3_{i+1;i} + \sum_{k=i+1}^{n_\rho} \gamma_{k,j} \left(\Delta^3_{k+1;i} - \Delta^3_{k+1;i+1} + \Delta^3_{k;i+1} - \Delta^3_{k;i} \right) \right] \end{aligned}$$

with $\Delta^3_{\ell;m} \equiv (r_\ell^2 - r_m^2)^{3/2}$

➽ Can compute $\bar{n}_{i,j}$ analytically!

Reconstruction

For the *j*th energy bin, the reconstruction works as follows:

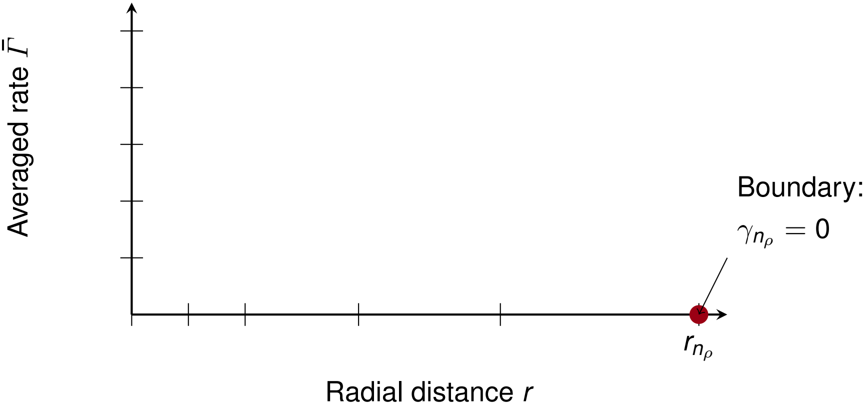

For the jth energy bin, the reconstruction works as follows:

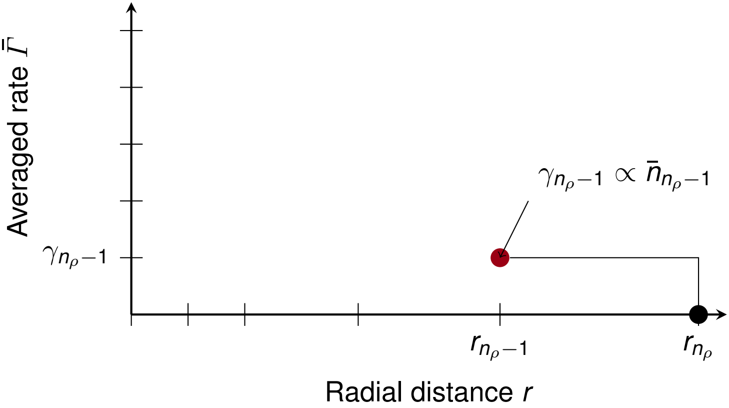

Reconstruction

For the *j*th energy bin, the reconstruction works as follows:

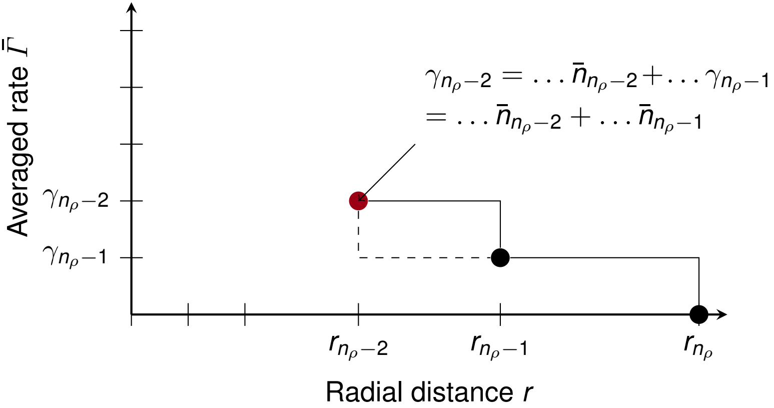

Reconstruction

For the jth energy bin, the reconstruction works as follows:

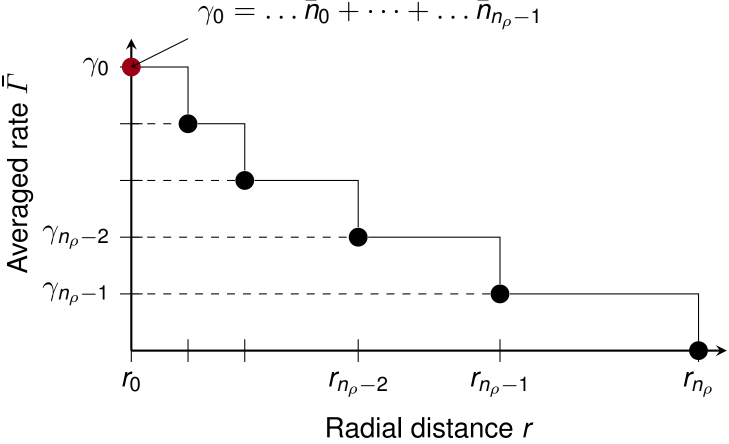

A simple reconstruction example

We write this as a matrix equation $\bar{n}_{i,j} = \sum_{k=1}^{n_\rho} \mathcal{M}_{ik}\, \gamma_{k,j}$ with

$$\mathcal{M}_{ik} \propto \begin{cases} \mathit{\Delta}^3_{i+1;i} & \text{for } i = k, \\ \mathit{\Delta}^3_{k+1;i} - \mathit{\Delta}^3_{k+1;i+1} + \mathit{\Delta}^3_{k;i+1} - \mathit{\Delta}^3_{k;i} & \text{for } k > i, \\ 0 & \text{otherwise.} \end{cases}$$

A simple reconstruction example

We write this as a matrix equation $\bar{n}_{i,j} = \sum_{k=1}^{n_\rho} \mathcal{M}_{ik}\, \gamma_{k,j}$ with

$$\mathcal{M}_{ik} \propto \begin{cases} \Delta^3_{i+1;i} & \text{for } i = k, \\ \Delta^3_{k+1;i} - \Delta^3_{k+1;i+1} + \Delta^3_{k;i+1} - \Delta^3_{k;i} & \text{for } k > i, \\ 0 & \text{otherwise.} \end{cases}$$

➽ Triangular matrix: set expected = observed counts, invert

$$n_{i,j} = \mathcal{M}_{ii}\gamma_{i,j} + \sum_{k=i+1}^{n_\rho} \mathcal{M}_{ik}\, \gamma_{k,j} \Rightarrow \gamma_{i,j} = \frac{1}{\mathcal{M}_{ii}} \left(n_{i,j} - \sum_{k=i+1}^{n_\rho} \mathcal{M}_{ik}\, \gamma_{k,j} \right)$$

A simple reconstruction example

We write this as a matrix equation $\bar{n}_{i,j} = \sum_{k=1}^{n_\rho} \mathcal{M}_{ik}\,\gamma_{k,j}$ with

$$\mathcal{M}_{ik} \propto \begin{cases} \Delta^3_{i+1;i} & \text{for } i = k, \\ \Delta^3_{k+1;i} - \Delta^3_{k+1;i+1} + \Delta^3_{k;i+1} - \Delta^3_{k;i} & \text{for } k > i, \\ 0 & \text{otherwise.} \end{cases}$$

➽ Triangular matrix: set expected = observed counts, invert

$$n_{i,j} = \mathcal{M}_{ii}\gamma_{i,j} + \sum_{k=i+1}^{n_\rho} \mathcal{M}_{ik}\,\gamma_{k,j} \Rightarrow \gamma_{i,j} = \frac{1}{\mathcal{M}_{ii}}\left(n_{i,j} - \sum_{k=i+1}^{n_\rho} \mathcal{M}_{ik}\,\gamma_{k,j}\right)$$

➽ Can also propagate errors; use when fitting $g_{a\gamma}$, T_i and κ_i

$$\sigma^2_{i,j} \equiv (\Delta\gamma_{i,j})^2 = \frac{1}{\mathcal{M}^2_{ii}}\left[n_{i,j} + \sum_{k=i+1}^{n_\rho} \mathcal{M}^2_{ik}\,\sigma^2_{k,j}\right]$$

Reconstruction in practice

- We want a closer approx. of $T(r) \Rightarrow$ splines? Sadly: ringing!
- Matrix invertible only if $n_{i,j} \neq 0 \Rightarrow$ uneven bin sizes

Reconstruction in practice

- We want a closer approx. of $T(r) \Rightarrow$ splines? Sadly: ringing!
- Matrix invertible only if $n_{i,j} \neq 0 \Rightarrow$ uneven bin sizes

➽ Choose direct fitting approach: general (shape-preserving) spline interpolation, compute integral again:

$$\bar{\Gamma}_j^{\mathrm{P}}(r) = \sum_i \left[\gamma_{i,j} + \sum_{k=1}^{3} c_{k;i,j}(r - r_i)^k\right] \Theta(r - r_i)\, \Theta(r_{i+1} - r)\,.$$

Reconstruction in practice

- We want a closer approx. of $T(r) \Rightarrow$ splines? Sadly: ringing!
- Matrix invertible only if $n_{i,j} \neq 0 \Rightarrow$ uneven bin sizes
- Choose direct fitting approach: general (shape-preserving) spline interpolation, compute integral again:

$$\bar{\Gamma}_j^{\mathrm{P}}(r) = \sum_i \left[\gamma_{i,j} + \sum_{k=1}^{3} c_{k;i,j}(r - r_i)^k\right] \Theta(r - r_i)\,\Theta(r_{i+1} - r)\,.$$

- Problem: matrix not square, no inversion; need to directly fit $g_{a\gamma}$, T_i and κ_i to the $n_{i,j}$:

$$\Delta\chi^2 \equiv -2\log L(g_{a\gamma},\,\{\kappa_i,\ T_i\}) = 2\sum_j \bar{n}_{i,j} - n_{i,j}\,\log(\bar{n}_{i,j})$$

Results

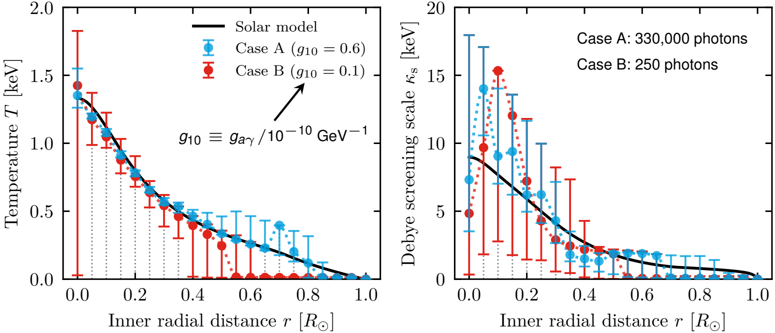

- Accurate $T(r)$ reconstruction up to $0.5\,\mathrm{R}_\odot$ ($0.8\,\mathrm{R}_\odot$)

Results

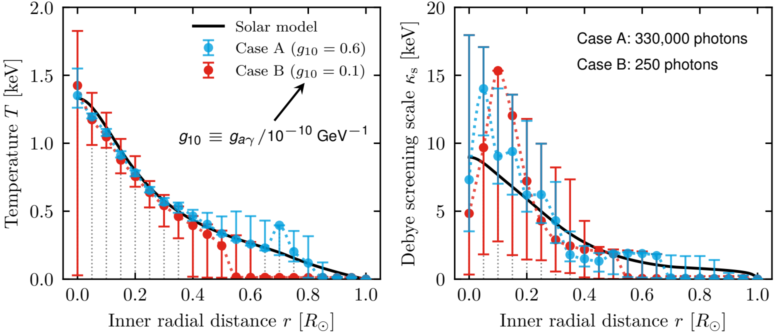

- Accurate $T(r)$ reconstruction up to 0.5 $\mathrm{R}_\odot$ (0.8 $\mathrm{R}_\odot$)
- Expected median stat. errors of 10% (16%)
- Difficulties for κ_s: shallow minima, weaker functional dependence, approximation used for Γ^{P}

Could we do the same reconstruction using neutrinos?

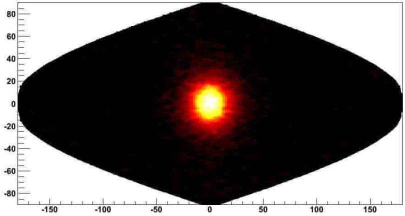

Super-K Collaboration 1998–2018

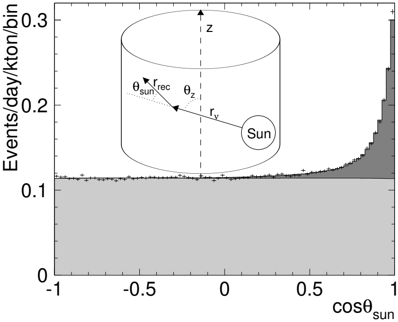

1606.07538

Solar ν image with more than 10^5 events!

Reconstruct $T(r)$ with νs?!

Could we do the same reconstruction using neutrinos?

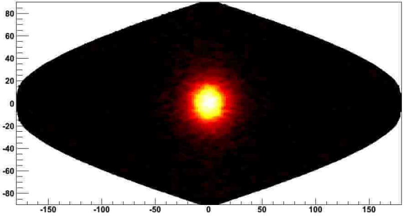

Super-K Collaboration 1998–2018

Solar ν image with more than 10^5 events!

Reconstruct $T(r)$ with νs?!

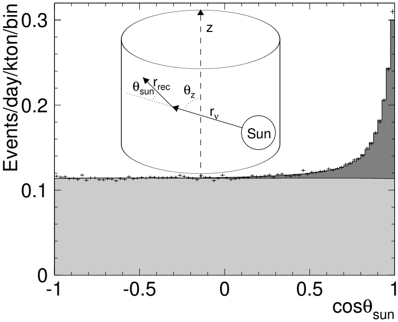

1606.07538

No. Angular resolution $\sim 40^\circ$ vs the Sun's apparent size $\sim 0.5^\circ$, e^- recoil and ν path not aligned

➽ Helioscope X-ray optics offer superior spatial resolution

Summary

- Primakoff flux predicted at percent level $\Rightarrow$ detection in IAXO = use axions as messengers for solar physics
- Accurate, model-independent(!) reconstruction of solar temperature profile $T(r)$ with axions is possible
- Axion tomography with helioscopes would benefit from great X-ray optics
- Growing public software framework for solar axions (and other WISPs?) within MSCA project "AxiTools"

Three different reconstruction techniques